

Electronic Supplementary Information

Magnetic forces produced by rectangular permanent magnets in static microsystems

*Anne-Laure Gassner^a, Mélanie Abonnenc^a, Hong-Xu Chen^b, Jacques Morandini^c, Jacques
Josserand^a, Joël S. Rossier^d, Jean-Marc Busnel^a and Hubert H. Girault^{*a}*

^aLaboratoire d'Electrochimie Physique et Analytique, EPFL SB ISIC LEPA, Lausanne, Switzerland

^bBeijing National Laboratory for Molecular Sciences, College of Chemistry Peking University, Beijing, China

^cAstek Rhone-Alpes, 1 place du Verseau, 38130 Echirolles, France

^dDiagnoSwiss SA, 2 Route de l'Ile-au-Bois, 1870 Monthey, Switzerland

ESI 1: Detailed explanation of the $(\mathbf{B} \cdot \nabla)\mathbf{B}$ part of the magnetic force

The magnetic force was already expressed in Equation 3. This paragraph aims at explaining how to deal with the $(\mathbf{B} \cdot \nabla)\mathbf{B}$ term. In 2D conditions, the matrix expressing the different components of the force reduces to the 2x2 matrix presented below:

$$\mathbf{F}_m = \frac{V\chi}{\mu_0} \begin{pmatrix} \mathbf{B}_x \frac{\partial \mathbf{B}_x}{\partial x} & \mathbf{B}_y \frac{\partial \mathbf{B}_x}{\partial y} \\ \mathbf{B}_x \frac{\partial \mathbf{B}_y}{\partial x} & \mathbf{B}_y \frac{\partial \mathbf{B}_y}{\partial y} \end{pmatrix} \quad (\text{S1})$$

The first line of the matrix corresponds to the x component of the force, and the second to the y component. So, for each component of the force, four variables relative to the matrix take part to the building of the force. The two components can be written as:

$$\left. \begin{aligned} \mathbf{F}_x &= \frac{V\chi}{\mu_0} \left(\mathbf{B}_x \frac{\partial \mathbf{B}_x}{\partial x} + \mathbf{B}_y \frac{\partial \mathbf{B}_x}{\partial y} \right) \\ \mathbf{F}_y &= \frac{V\chi}{\mu_0} \left(\mathbf{B}_x \frac{\partial \mathbf{B}_y}{\partial x} + \mathbf{B}_y \frac{\partial \mathbf{B}_y}{\partial y} \right) \end{aligned} \right\} \quad (\text{S2})$$

The volume of the bead, its magnetic susceptibility and the permeability of the free space being constant in our simulations, the force will be determined by the matrix elements. All these elements have been plotted at different places (zones) in the microchannel. These zones are defined in Figure S1 (left). The attraction configuration, with the reference numerical parameters described in the article ($h=l=s= 200 \mu\text{m}$, microchannel height = $100 \mu\text{m}$, insulating layer height = $50 \mu\text{m}$), has been considered as an example. As a reminder the vector representation of the magnetic force is also presented in Figure S1 (right).

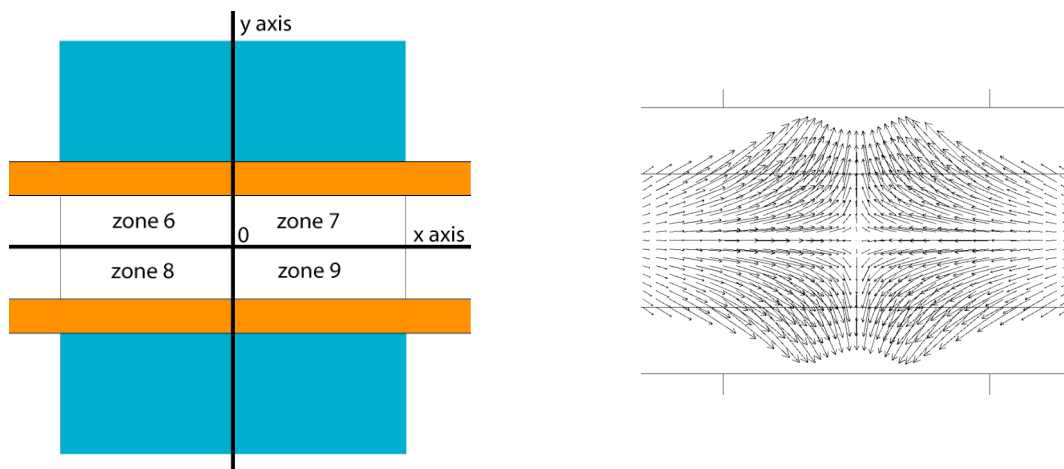


Figure S1: left: scheme of the different zones. The microchannel is closed by two insulating layers (orange) and placed between two permanent magnets (blue). Right: vector representation of the magnetic force \mathbf{F} for the attraction configuration

Three ways through the microchannel, parallel to the x -axis, have been considered: one at $y=0$, one at $y=25\ \mu\text{m}$ and the last at $y=-25\ \mu\text{m}$ (corresponding to $\pm 1/4$ of the microchannel, its height being $100\ \mu\text{m}$). In the same manner three ways have been drawn parallel to the y -axis: one at $x=0$, the second at $x=50\ \mu\text{m}$ and the last one at $x=-50\ \mu\text{m}$ ($\pm 1/4$, the length of the magnets being $200\ \mu\text{m}$). The x and y components of \mathbf{B} have been plotted for each way. Due to symmetry, some curves are superimposed. All the curves are presented in Figure S2, with in (a) the ways along the x -axis and in (b) the ways along the y -axis.

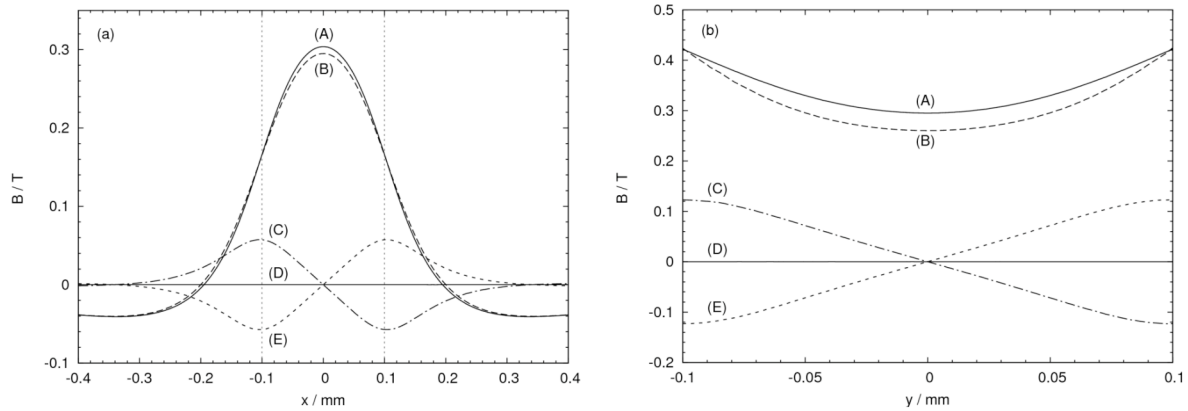


Figure S2: Curves representing the x and y components of B depending on the position in the microchannel (attraction configuration). The vertical dashed lines show the magnets position. (a) ways along the x -axis with (A) B_y at $y = \pm 25\ \mu\text{m}$, (B) B_y at $y = 0$, (C) B_x at $y = +25\ \mu\text{m}$, (D) B_x at $y = 0$ and (E) B_x at $y = -25\ \mu\text{m}$. (b) ways along the y -axis with (A) B_y at $x = 0$, (B) B_y at $x = \pm 50\ \mu\text{m}$, (C) B_x at $x = +50\ \mu\text{m}$, (D) B_x at $x = 0$ and (E) B_x at $x = -50\ \mu\text{m}$.

Using the values and slopes of the curves of Figure S2, it is possible to determine the sign or value of each component involved in the magnetic force. The values obtained are summarized in Table S1. The values for point (0,0) are determined in the following way: from curve (D) of Figure S2a, B_x is equal to zero at point (0,0). From curve (B) of Fig. S2a, B_y has a positive value at point (0,0). As B_x is equal to zero on the x -axis (Fig. S2a (D)), its derivative relative to x is inevitably equal to zero. As B_x is equal to zero on the y -axis (Fig. S2b (D)), its derivative relative to y is as well equal to zero. By definition, the slope of a maxima or minima is equal to zero, such as the derivative of B_y relative to x (curve (B) of Fig. S2a) is equal to zero. The same argument can be applied to the last term (curve (A) of Fig. S2b). By multiplying the different elements according to Equations S2, the sign of the magnetic force can be determined.

Table S1: sign of the component in a definite zone.

	B_x	B_y	$\frac{\partial B_x}{\partial x}$	$\frac{\partial B_x}{\partial y}$	$\frac{\partial B_y}{\partial x}$	$\frac{\partial B_y}{\partial y}$	F_x	F_y
Point (0,0)	0	+	0	0	0	0	0	0
Negative x-axis (between dashed lines)	0	+	0	+	+	0	+	0
Positive x-axis (between dashed lines)	0	+	0	-	-	0	-	0
Positive y-axis	0	+	-	0	0	+	0	+
Negative y-axis	0	+	+	0	0	-	0	-
Zone 6	+	+	-	+	+	+	+	+
Zone 7	-	+	-	-	-	+	-	+
Zone 8	-	+	+	+	+	-	+	-
Zone 9	+	+	+	-	-	-	-	-

ESI 2: Finite-element formulation

The integral formulation is based on the local form (S3), coming from equation (5) of the paper, presented here in the general situation ($\mu \neq \mu_0$), where $\mathbf{B}_0 = \mu_0 \mathbf{M}_0$ is the magnetic flux density vector imposed in the magnet:

$$\nabla \cdot (-\mu \nabla \phi + \mathbf{B}_0) = 0 \quad (\text{S3})$$

Equation (S3) is derived in the global form (S4), using the Galerkin formulation frequently used in the finite element method (multiplication by a projective function α and integration on the domain of study, W). Note that all the gradients are written in the nabla form ∇ .

$$\iint_W \alpha [\nabla \cdot (-\mu \nabla \phi + \mathbf{B}_0)] dW = 0 \quad (\text{S4})$$

By decomposing the product between α and the divergence in (S4), the second order derivative of the unknown ϕ (divergence of $\nabla \phi$) becomes:

$$\alpha \nabla \cdot (-\mu \nabla \phi) = \nabla \cdot (-\alpha \mu \nabla \phi) + \mu \nabla \alpha \cdot \nabla \phi \quad (\text{S5})$$

Injecting (S5) in (S4) and using the Ostrogradsky theorem, the divergence term (second term of (S5)) is rejected at the boundary where it equals to zero (no magnetic field crossing the external boundaries of the domain):

$$\iint_W [\mu \nabla \alpha \cdot \nabla \phi + \alpha \mathbf{B}_0] dW = 0 \quad (\text{S6})$$

Using the function β for the interpolation of the unknown vector ϕ (of the same kind as the projective function α), we obtain the final form (S7) where the first term corresponds to the matrix to invert, multiplied by the unknown vector ϕ , the second term being the source term:

$$\iint_W [(\mu \nabla \alpha \cdot \nabla \beta) \phi + \alpha \mathbf{B}_0] dW = 0 \quad (\text{S7})$$

ESI 3: Validation of the air box and mesh size for the reference square magnet (200 μm)

The influence of different parameters was evaluated, such as to validate the simulation conditions. The first one is the size of the air box, that is to say the parameters designing the vertical air space between the top of the magnet and the beginning of the infinite air layer (h_{air}) and the horizontal air space between the end of the microchannel and the beginning of the infinite air layer (l_{air}), showed in Figure 1 of the paper. One parameter is varied at once. The greatest value of each parameter is chosen as reference. The results are presented in Table S2. The last line presents the chosen values of the system. It can be seen that varying these parameters doesn't induce a noteworthy error. Our tolerance accepts values until a 0.2 % error, allowing all the values of the table. It shows the great usefulness of the infinite air layer that limits greatly the error.

Table S2: evaluation of the error on the magnetic flux density according to the air box parameters h_{air} and l_{air}

$h_{air} / \mu\text{m}$	$l_{air} / \mu\text{m}$	B_x / T	Error / %	B_y / T	Error / %
500	500	2.07142E-1	-	4.61066E-1	-
400	500	2.07171E-1	0.0140	4.61459E-1	0.0852
300	500	2.07183E-1	0.0198	4.61197E-1	0.0284
200	500	2.07186E-1	0.0212	4.60829E-1	0.0514
100	500	2.07158E-1	0.0077	4.61316E-1	0.0542
500	400	2.0718E-1	0.0183	4.60816E-1	0.0542
500	300	2.0718E-1	0.0183	4.61640E-1	0.1245
500	200	2.07166E-1	0.0116	4.61592E-1	0.1141
500	100	2.07161E-1	0.0092	4.61421E-1	0.0770
300	300	2.07234E-1	0.0444	4.61141E-1	0.0163

The mesh size of the middle of the channel (that is to say the part comprised between the magnets) was then evaluated. The smallest mesh size was chosen as reference. It is also the value chosen for the system. Table S3 presents the results obtained. Again it can be seen that the error is always under 0.2%, allowing the use of all the values. The finest meshing was chosen, because the middle of the microchannel is the region of interest and the calculation of the magnetic force requires precise values of B .

Table S3: evaluation of the error on the magnetic flux density according to the mesh size in the middle of the microchannel. Mesh size of point coordinates (in μm) $(-100,0)/(100,0)/(0,0)/(-100,50);(-100,-50);(100,50)$ and $(100,-50)$

Mesh size / μm	B_x / T	Error / %	B_y / T	Error / %
3/3/5/7	2.07234E-1	-	4.61141E-1	-
5/5/5/7	2.07195E-1	0.0188	4.61066E-1	0.0163
7/7/7/7	2.07132E-1	0.0492	4.61282E-1	0.0306
10/10/10/10	2.07460E-1	0.1091	4.61252E-1	0.0241

The last parameter is the mesh size of the magnets, more precisely their corners. Table S4 presents the results obtained, showing again errors under 0.2% except for the mesh size of 25 μm , allowing the choice of all the other values. Our system used a mesh size of 10 μm .

Table S4: evaluation of the error on the magnetic flux density according to the mesh size of the magnets corners

Mesh size / μm	B_x / T	Error / %	B_y / T	Error / %
7	2.07229E-1	-	4.61004E-1	-
10	2.07234E-1	0.0024	4.61141E-1	0.0297
15	2.07181E-1	0.0232	4.61577E-1	0.1243
20	2.07172E-1	0.0275	4.61613E-1	0.1319
25	2.07133E-1	0.0463	4.63877E-1	0.6232

ESI 4: Validation of the numerical model

The present work was validated by comparison with the work of Bronzeau et al, who used the software FEMM 4.0 to simulate the 2D magnetic field produced by two NdFeB magnets (5 mm high and 2 mm long) in attraction configuration with a spacing of 0.5 mm. The model presented simulated the same system.

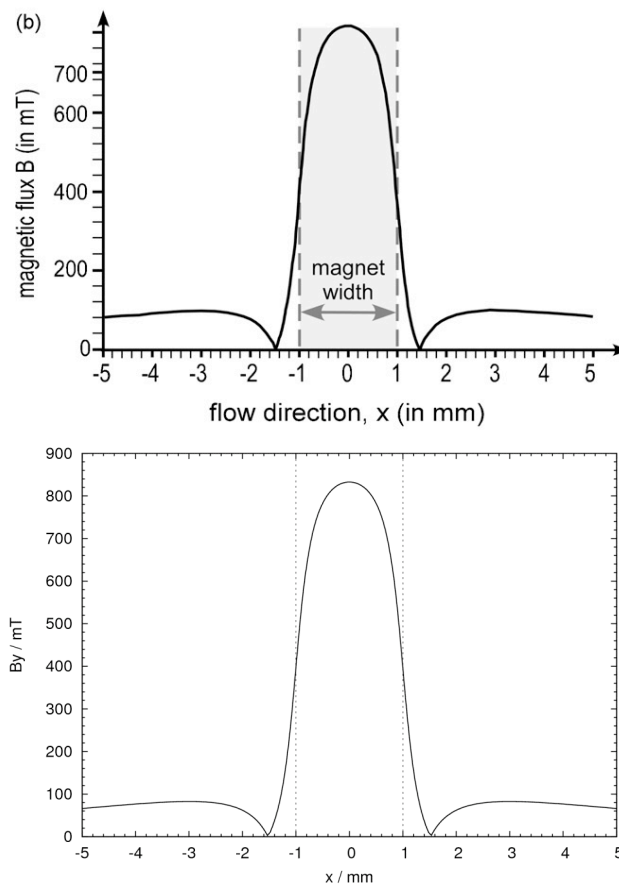


Figure S3: comparison of the two models. On the top: FEMM 4.0, on the bottom: the model presented. For clarity reasons, the magnetic flux density was plotted as an absolute value

Figure S3 presents the plot of the y component of the magnetic flux density along the x axis, in the middle of the microchannel. It can be seen that the shape of the curve is very similar, as well as the zero and maximum values. This good adequation validates the model presented.

ESI 5: Effect of the magnet size on B_y in the magnet

This effect was already shown in Figure 5a. The magnitude of the magnetic flux density y component varies with the l/s ratio. Figure 5a showed this effect for a point near the microchannel (black dot in Figure S4 left). Figure S4 shows the same effect for two other points placed on the x symmetry axis of the magnet.

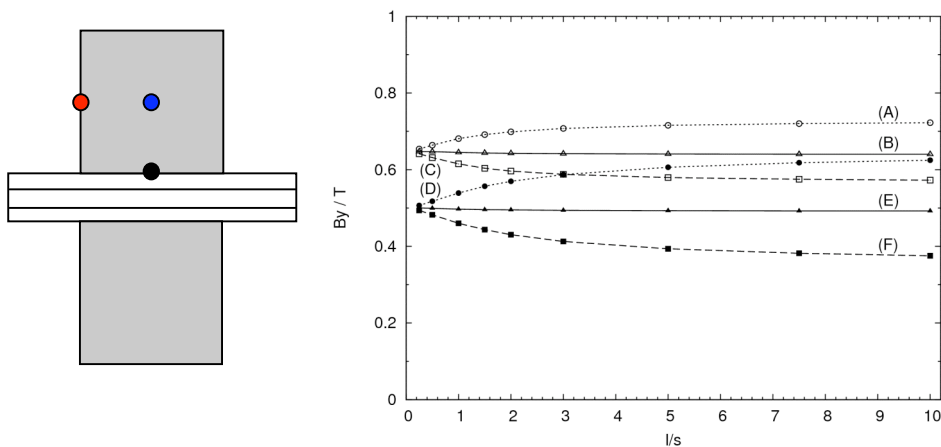


Figure S4: Behaviour of the magnetic flux density (y component) for square magnets in function of l/s , with s constant ($s = 200 \mu\text{m}$). Values taken at the red dot (left scheme): (A) attraction, (B) single magnet and (C) repulsion. Values taken at the central point of the magnets (blue dot): (D) attraction, (E) single magnet and (F) repulsion.

The behaviour is similar to what was observed in Figure 5a. When the value of the l/s ratio is low, the three configurations are nearly equal. Upon increasing the ratio, the value for the single magnet configuration remains constant, whereas the value for attraction and repulsion increases and decreases respectively. Moreover Figure S4 shows that the l/s ratio has less influence in the center of the magnet (blue dot) than near the lower boundary (black dot, Figure 5a). It can also be seen that the effect is less strong near the left (and by symmetry right) boundary.

ESI 6: Effect of magnets spacing for square magnets

To complete this study, the influence of the magnets spacing is treated for square magnets. The system was first simulated for micrometer-sized magnets (h and $l = 200 \mu\text{m}$), and then for millimeter-sized magnets (h and $l = 2 \text{ mm}$). The parameter s was modified and the resulting magnetic force plotted along a horizontal path (x -axis). Figure S5 presents the magnetic force obtained for micromagnets.

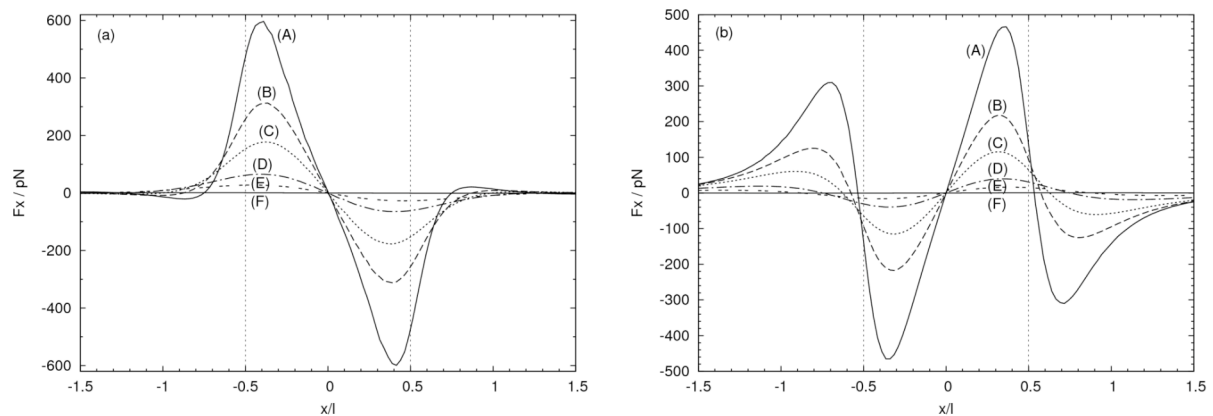


Figure S5: Variation of the magnetic force (x component) in function of s for square magnets with constant dimensions ($h=l= 200 \mu\text{m}$). The force was calculated for a bead of $1 \mu\text{m}$ diameter and unit susceptibility. The values are taken along a horizontal path (x -axis). The vertical dashed lines show the magnets position. (a) attraction and (b) repulsion. $s =$: (A) $100 \mu\text{m}$, (B) $150 \mu\text{m}$, (C) $200 \mu\text{m}$, (D) $300 \mu\text{m}$, (E) $400 \mu\text{m}$ and (F) $1000 \mu\text{m}$.

It can be seen that the magnetic force logically decreases as the spacing increases: the further the magnets are, the smaller is the force. For a spacing of $1000 \mu\text{m}$ already, the magnetic force is nearly equal to zero. Consequently, the magnets should be placed as near from the microchannel as possible to obtain a high force.

Figure S6 shows the effect of the spacing for millimeter-size magnets. Again the force decreases when the spacing increases. By comparison with Figure S5, it can be seen that the spacing for which the force is nearly equal to zero is larger for millimeter-size magnets than for micromagnets.

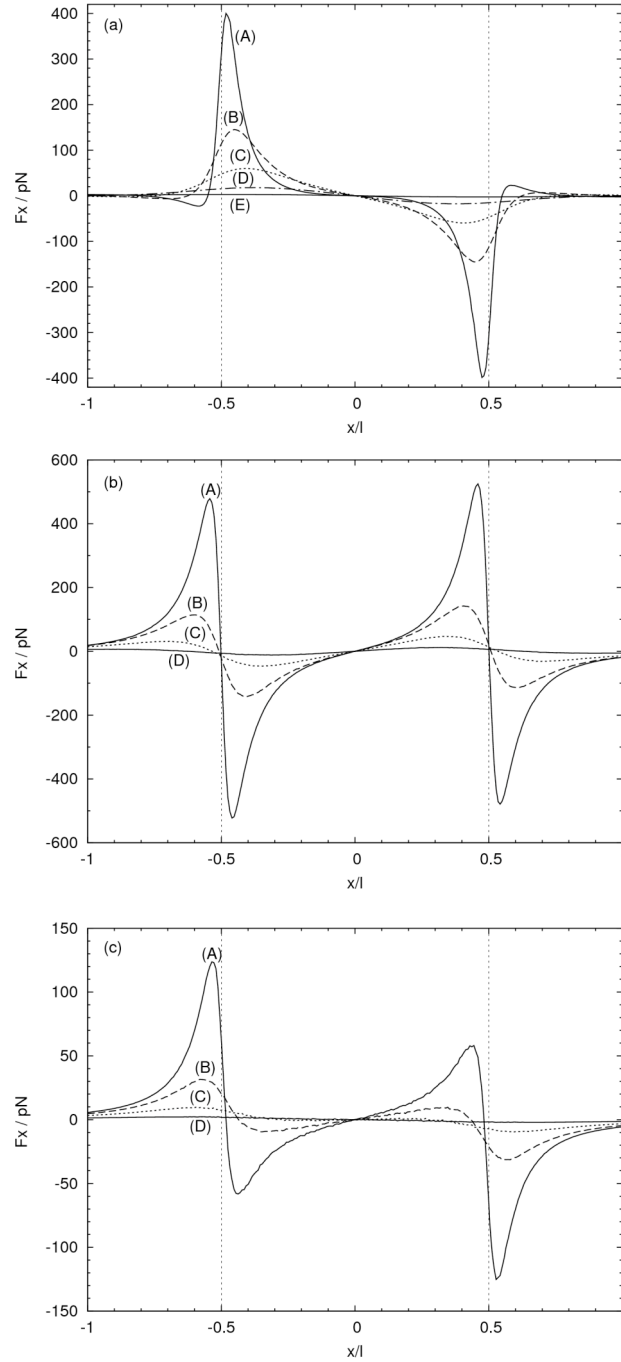


Figure S6: Variation of the magnetic force (x component) in function of s for square magnets with constant dimensions ($h=l= 2 \text{ mm}$). The force was calculated for a bead of $1 \mu\text{m}$ diameter and unit susceptibility. The values are taken along a horizontal path (x axis). The vertical dashed lines show the magnets position. (a) attraction, (b) repulsion and (c) single magnet. $s =$: (A) $200 \mu\text{m}$, (B) $500 \mu\text{m}$, (C) $1000 \mu\text{m}$, (D) $2000 \mu\text{m}$ and (E) $4000 \mu\text{m}$.

As a conclusion, the larger the spacing is, the smaller the magnetic force. The magnets should be placed as close to the microchannel as possible. With larger magnets than presented, the spacing can have a higher value, but it should be kept as small as possible.